ACTA ACUSTICA UNITED WITH ACUSTICA
Vol. 98 (2012) 567 – 576

DOI 10.3813/AAA.918538

Biot Effects for Sound Absorbing Double Porosity Materials

O. Dazel[1)], F.-X. Bécot[2)], L. Jaouen[2)]

[1)] Laboratoire d'Acoustique de l'Université du Maine - UMR CNRS 6613, Avenue Olivier Messiaen, 72 085 Le Mans Cedex, France. olivier.dazel@univ-lemans.fr

[2)] Matelys - Acoustique & Vibrations, 1 rue Baumer, 69120 Vaulx-en-Velin, France

Summary

In this paper, a model for sound propagation in double porosity materials with elastic frame is proposed. The main originality of this paper is to develop a model which is suitable for sound absorbing materials. The original idea is to replace the fluid-phase related properties of a single porosity material in Biot transverse isotropic equations with those of a double porosity medium. The model is then developed for 1D problem and used to derive the surface impedance and the sound absorption coefficient of double porosity samples. To quantify the influence of the porous sample dimensions, a numerical procedure based on a finite element simulations is proposed. It is applied to perforated porous samples (a polymer foam and one fibrous material with two different size of perforation) subject to a plane wave at normal incidence. Numerical results are compared to impedance tube measurements.

PACS no. 43.20.Bi, 43.20.El, 43.20.Fn, 43.20.Ye

1. Introduction

Porous materials are widely used for sound proofing packages in automotive, transportation and building acoustics. Due to their morphology, these materials are efficient in the mid to high frequency ranges but exhibit weak performances for low frequencies. Hence, sound absorption at frequencies lower than 500 Hz is often very low for material samples thinner than 50 mm. To overcome this lack of efficiency for practical applications, several solutions have been proposed in the last decade. One idea is to use multilayered systems in order to improve the global acoustic performance. In order to control and to optimize the performances, theories [1, 2] have been proposed to predict the response of multilayered sound packages. These packages lead to configurations whose thicknesses is generally around 10–15 cm which is close to the quarter wavelength. The concept of mass-spring systems which consists of a porous material covered by a heavy layer or a perforated plate [3, 4, 5] could allow a good sound absorption at very low frequencies limited however to a narrow frequency band. Alternatively, hybrid solutions [6, 7, 8] have been developed which include porous materials for the mid to high frequency range and a separate active control system to act at low frequencies. These promising solutions however require external supplies which increase the cost of the treatment and the resulting electrical power may restrain the applications only to gentle environmental conditions.

In this work double porosity materials are considered[9, 10, 11, 12] which where originaly studied for geophysical applications. Double porosity materials contain two pore networks, the characteristic sizes of which are separated at least by an order of magnitude. In this work, the smaller size pores are called micropores and the larger ones are denoted by mesopores. Pioneering works by Boutin *et al.* [13] and Olny & Boutin [14] have revealed the potential of these materials to design passive sound absorbing solutions with good performances at low frequencies. The added absorption effect is due to to a partial coupling between the acoustic fields in the two pore networks. Subsequent works [15, 16, 17] have shown that double porosity materials in the form of perforated porous materials could be designed to select the frequency range of maximum efficiency and they are compliant with the use of highly resistive or impervious screens.

Models for sound propagation in rigid frame double porosity materials have been proposed [13, 14], based on homogenization theory[18, 19]. They are concerned with materials of infinite dimension and they model double scale materials as equivalent fluids in which one compressional wave propagates. For sound absorbing materials, properties (density $\widetilde{\rho}_{dp}$ and compressibility $\widetilde{K}_{dp}$ in which subscript *dp* refers to double porosity quantities) of the homogenized medium were given by Olny and Boutin [14] as frequency dependent functions taking into account viscous, thermal and pressure diffusion effects. More precisely, it was shown that the macroscopic descriptions

Received 2 March 2011,
accepted 27 February 2012.

depend on the contrast with static permeability between pores and micropores. Consequently, two main macroscopic behaviors were proposed (low and high permeability contrast).

Generally a good agreement with measurements was demonstrated [20, 16]. However, notable discrepancies have been observed in in some cases. Even if some noticeable discrepancies can be observed. In Figure 6 of [16], a frame resonance is observed around 1400 Hz which corresponds to the porous frame deformation neglected in the homogenized equivalent fluid model [14]. In addition the semi-analytical model proposed in this paper underestimates the absorption beyond 1200 Hz. Similar comments can be made about the results presented in Figure 5 of [20] and on those proposed in the present work. The rigid frame assumption was intrinsically linked to the model. Olny mentioned in his original work [21] that finite-size dimensions should lead to a modification of the model parameters but without entering into details.

All of these works focus on the rigid frame assumption which restrain the application of double porosity materials modeling to situations where they are rigidly backed. Models do not account for the coupling with flexible structures, which is the case in most of the vibro-acoutics practical applications. Note that possible inertia effects [22] may be accounted for in double porosity materials [17]. The main goal of the present work is to adapt the Biot theory [23] to account for the frame deformation of double porosity materials. Auriault and Boutin [10, 11, 12] modeled of double porosity geomechanical materials with flexible frame and proposed equations which are, in one way, similar to the ones of the Biot theory. Nevertheless, the assumptions and the formalism were not adapted to sound absorption problems.

The Biot theory [23, 24] has shown its relevance to modeling acoustic propagation in single porosity sound absorbing materials with a deformable frame [25, 26]. The approach consists in modeling the porous material as the superposition of two continua: a solid and a fluid phase. Each one is described by a displacement field. A common point of all these representations is that the solid phase is modeled by its macroscopical displacement u^s. It is defined as the average of the microscopic solid displacement on the solid part of the Representative Elementary Volume (REV). The original formulation [23] considers the fluid displacement u^f which is the average of the microscopic fluid displacement on the fluid part of the REV. This representation was nevertheless not valid for inhomogeneous materials[24]. Fluid phase displacement u^f has been replaced by the relative flow $w = \phi(u^f - u^s)$, ϕ denoting the porosity, defined as the ratio of the fluid volume to the total volume of the REV. More recently Dazel *et al.* [27] proposed an equivalent representation to the modified formulation, valid for inhomogeneous materials, which considers the total displacement $u^t = u^s + w = (1-\phi)u^s + \phi u^f$. This formulation presents the advantage of simplifying the formalism and is used in this paper.

The basic idea of the model proposed in this work is inspired by Biot's assumption: the displacement of the solid part is uniform at the microscopic scale. It can then be shown that the fluid phase properties (frequency dependent density and compressibility) are not modified by the solid motion and then are the ones of the equivalent homogenized fluid medium. Moreover, with the total displacement formulation [27], the parameters of the model can be deduced from the equivalent fluid and *in-vacuo* solid properties only. The idea of this work is to introduce equivalent fluid double porosity models in Biot's equations. This work is only concerned by propagation in layered structures and the mesopores are supposed to be orthogonal to the sample interfaces.

An analytical expression for the normal incidence surface impedance is derived from which the absorption coefficient is deduced. Inverse Finite Element Method is used to deduce the equivalent fluid properties of double porosity medium. Contrary to majority of the semi-analytical models, the proposed model integrates the finite thickness and lateral surface dimensions of the material. The results are compared to experiments and a very good agreement is observed.

Section 2 presents the theoretical model based on a transverse isotropic formulation [28] of Biot's equations. A simplified one-dimensional problem is then deduced which allows comparison with the data for normally incident wave. Section 3 presents the inverse numerical procedure to obtain the *in-vacuo* solid and fluid parameters of the model. Section 4 presents the comparison with experimental results. Two types of microporous materials (one foam and one fibrous material) are considered in this work, the parameters of which have been obtained by dedicated characterisation techniques and are given in Table I. Experimental results are presented for three double porosity materials. One is made from foam (Named F) and two of them are made from the fibrous material (denoted by W1 and W2). Their properties can be found in Table II.

2. Theoretical part

2.1. Transverse Isotropic Biot model for single porosity materials

The problem is modeled in cartesian coordinates $\{x, y, z\}$. For homogeneous single porosity materials, the equations in $\{u^s, u^t\}$ representation have been proposed by Khurana *et al.* [28] for an anisotropy direction along z. They read

$$\nabla\cdot\hat{\boldsymbol{\sigma}}^s(u^s) = -\omega^2\left[\tilde{\rho}_s\right]u^s - \omega^2\left[\widetilde{\gamma}\right]\left[\tilde{\rho}_{eq}\right]u^t, \tag{1a}$$

$$\widetilde{K}_{eq}\ \nabla\cdot\left(\ \nabla\cdot u^t\,\mathbb{I}\right) = -\omega^2\left[\widetilde{\gamma}\right]\left[\tilde{\rho}_{eq}\right]u^s - \omega^2\left[\tilde{\rho}_{eq}\right]u^t. \tag{1b}$$

$\hat{\boldsymbol{\sigma}}^s$ is the *in-vacuo* stress tensor of the solid phase and the stress-strain relations are

$$\hat{\sigma}_{xx} = 2N\varepsilon_{xx} + A\left(\varepsilon_{xx} + \varepsilon_{yy}\right) + F\varepsilon_{zz},$$

Table I. Values of the acoustic, elastic and damping parameters of the materials.

	σ	ϕ	α_∞	Λ	Λ'	k'_0	E	η_s	ν	ρ_1
Foam (see F)	93 500	0.96	3.32	15	50	15	260	0.5	0.33	42
Fibrous (see W1 and W2)	88 400	0.97	1.01	23	51	13	5 500	0.3	0	156
Fibrous (uncertainties)	±1600	±0.01	±0.2	±2.4	±5.7	±6.4	Ø	Ø	Ø	Ø
Units	N.s.m^{-4}	-	-	10^{-6} m	10^{-6} m	10^{-10} m^2	10^3 Pa	-	-	kg.m^{-3}

$$\hat{\sigma}_{yy} = 2N\varepsilon_{yy} + A(\varepsilon_{xx}+\varepsilon_{yy}) + F\varepsilon_{zz}, \tag{1c}$$
$$\hat{\sigma}_{zz} = C\varepsilon_{zz} + F(\varepsilon_{xx}+\varepsilon_{yy}), \qquad \hat{\sigma}_{yz} = 2L\varepsilon_{yz},$$
$$\hat{\sigma}_{xz} = 2L\varepsilon_{xz}, \qquad \hat{\sigma}_{xy} = 2N\varepsilon_{xy}.$$

A, N,F C and L are the *in-vacuo* elastic coefficients [28]. $\widetilde{K}_{eq}$ is the compressibility of the homogenized fluid phase. The interstitial pressure p is given by

$$p = -\widetilde{K}_{eq}\ \nabla\cdot u^t \tag{1d}$$

$[\widetilde{\gamma}]$, $[\widetilde{\rho}_s]$ and $[\tilde{\rho}_{eq}]$ are diagonal matrices [28]. For the purpose of this work, they are rewritten in the following form:

$$[\widetilde{\gamma}] = \rho_0[\tilde{\rho}_{eq}]^{-1} - (1-2\phi)[\mathbb{I}], \tag{1e}$$
$$[\widetilde{\rho}_s] = (1-\phi)\rho_s[\mathbb{I}] - (\rho_0[\mathbb{I}] - \phi[\tilde{\rho}_{eq}])(2\phi[\mathbb{I}] - \rho_0[\tilde{\rho}_{eq}]^{-1}). \tag{1f}$$

ρ_0 is the density of the saturating fluid, ρ_s is the density of the frame material. $[\mathbb{I}]$ is the identity matrix. The values of the diagonal terms of the $[\tilde{\rho}_{eq}]$ are associated to the densities of the homogenized equivalent fluid model and can be given by semi-phenomenological models [28, 26]. All the parameters of equations (1a-b) can then be obtained from the *in-vacuo* mechanical parameters (1c), $\widetilde{K}_{eq}$, $[\tilde{\rho}_{eq}]$, ρ_s, ρ_0 and porosity ϕ.

2.2. Transverse Isotropic Biot model for double porosity media

In the case of double porosity material, based on the assumptions of Biot's theory. The possible frame deformation does not influence the visco-thermal dissipation inside the double porosity material. In this framework, parameters of equations (1) should be replaced by analogues for the double porosity medium. A summary of the substitutions is given in Table III. The material is supposed to be homogenizable under the same assumptions as the ones of Olny and Boutin [14]. The REV Ω is then divided into three parts Ω_s, Ω_f and Ω_p respectively associated to the solid, fluid part of the microporous domain and the mesopore volume. Let V be the volume function. Let $\phi_m = V(\Omega_f)/V(\Omega_s \cup \Omega_f)$ be the porosity of a single porosity material and $\phi_p = V(\Omega_p)/V(\Omega)$ the porosity of the mesopores. The mesopore is supposed to be aligned with the x direction.

First, $\phi_{dp} = (1-\phi_p)\phi_m + \phi_p$ is the total porosity of the double porosity material (i.e. the ratio of the total volume of air to the total material one). The solid displacement field $u^s_{dp} = \}langleu^s_{mic}\rangle_{\Omega_s}$ is defined as the average microscopical displacement on Ω_s (*mic* index is associated to microscopical fields). For the fluid displacement u^f, one has

$$u^f_{dp} = \left\langle u^f_{mic}\right\rangle_{\Omega_p\cup\Omega_f} = \frac{\phi_p}{\phi_{dp}}\left\langle u^f_{mic}\right\rangle_{\Omega_p} + \frac{(1-\phi_p)\phi_m}{\phi_{dp}}\left\langle u^f_{mic}\right\rangle_{\Omega_f}. \tag{2}$$

The total displacement is defined as

$$u^t_{dp} = \underbrace{(1-\phi_p)(1-\phi_m)}_{1-\phi_{dp}} u^s_{dp} + \phi_{dp}u^f_{dp}. \tag{3}$$

ρ_0 and ρ_s in equations (1e-f) remain unchanged as they correspond to densities of air and of the frame material. It is generally common (even if unused in the present representation) to use the solid frame density ρ_1 which is the density of the porous solid and ρ_2 equivalent density of air. Their expressions are given in Table III. Assumption $u^s_{dp} = 0$ leads to the equivalent fluid model and u^t_{dp} is then the displacement of the homogenized medium. Parameters $\widetilde{\rho}_{eq}$ and $\widetilde{K}_{eq}$ of the equivalent fluid should then be respectively replaced by $\widetilde{\rho}_{dp}$ and $\widetilde{K}_{dp}$. Expressions of $[\widetilde{\gamma}^{dp}]$ and $[\widetilde{\rho}_s]$ are deduced from equations (1e-f) where ϕ (resp. $\widetilde{\rho}_{eq}$)

Table II. Double Porosity materials properties.

DP medium	Unit	F	W1	W2
Microporous material		Foam	Fibrous	Fibrous
Diameter	mm	46	100	100
Mesopore diameter	mm	9.5	35.7	43.6
Thickness	mm	23.8	80	80

Table III. Parameters for the porous medium. **: in each direction.

SP model	DP model
ϕ	$\phi_{dp} = (1-\phi_p)\phi_m + \phi_p$
u^s	u^s_m
u^t	$u^t_{dp} = (1-\phi_p)u^t_m + \phi_p u^p$
ρ_1	$\rho_1^{dp} = (1-\phi_p)\rho_1$
ρ_2	$\rho_2^{dp} = [\phi_p + (1-\phi_p)\phi_m]\rho_0$
$\widetilde{\rho}_{eq}$	$\widetilde{\rho}^{dp}_{eq} = \widetilde{\rho}_{dp}$ **
$\widetilde{\gamma}$	$\widetilde{\gamma}^{dp} = \rho_0/\tilde{\rho}^{dp}_{eq} - (1-2\phi_{dp})$ **
$\widetilde{\rho}_s$	$\widetilde{\rho}^{dp}_s = (1-\phi_{dp})\rho_s - (\rho_0 - \phi_{dp}\tilde{\rho}^{dp}_{eq}) \cdot(2\phi_{dp} - \rho_0/\tilde{\rho}^{dp}_{eq})$ **

should be replaced by ϕ_{dp} (resp. $\widetilde{\rho}_{dp}$). Elastic coefficients of constitutive law (1c) are also modified and their values will be investigated in section 3.

2.3. 1D propagation model

We focus on impedance tube measurements. We are interested by wave propagation along z axis and the equations of motion read

$$\underbrace{\left(C_{dp}+F_{dp}\right)}_{P_{dp}}\frac{\partial^2 u^s_{dp}}{\partial z^2} = -\omega^2\widetilde{\rho}_s^{dp}u^s_{dp} - \omega^2\widetilde{\gamma}^{dp}\widetilde{\rho}_{dp}\,u^t_{dp}, \tag{4a}$$

$$\widetilde{K}_{dp}\frac{\partial^2 u^t_{dp}}{\partial z^2} = -\omega^2\widetilde{\gamma}^{dp}\widetilde{\rho}_{dp}\,u^s_{dp} - \omega^2\widetilde{\rho}_{dp}\,u^t_{dp}. \tag{4b}$$

C_{dp} and F_{dp} are the Lamé coefficients along z-axis. This system is of Biot type and it can be shown that two compression waves can propagate. They are defined by their wave numbers k_i and the ratios $\mu_i = u^t_{dp}/u^s_{dp}$ which are given by [27]

$$k_i^2 = \frac{\left(k_{s2}^2+k_{dp}^2\right)+(-1)^i\sqrt{\left(k_{s2}^2+k_{dp}^2\right)^2-4k_{dp}^2k_{s1}^2}}{2}, \tag{5}$$

$i = 1, 2$, with

$$k_{dp} = \omega\sqrt{\frac{\widetilde{\rho}_{dp}}{\widetilde{K}_{dp}}}, \quad k_{s1} = \omega\sqrt{\frac{\widetilde{\rho}}{P_{dp}}},$$

$$k_{s2} = \omega\sqrt{\frac{\widetilde{\rho}_s}{P_{dp}}}, \quad \widetilde{\rho} = \widetilde{\rho}_s - (\widetilde{\gamma}^{dp})^2\widetilde{\rho}_{dp}. \tag{6}$$

In addition,

$$\mu_i = \widetilde{\gamma}^{dp}\frac{(k_i^2-k_{s2}^2)}{k_{s2}^2-k_{s1}^2} = \widetilde{\gamma}^{dp}\frac{k_{dp}^2}{k_i^2-k_{dp}^2}. \tag{7}$$

Normal incidence surface impedance of a layer of double porosity medium (thickness d) backed by a rigid wall can then be calculated. As shown in Figure 2, origin of z axis is fixed at the rigid backing. The displacement of solid phase and the total displacement can be expressed through the two compressional waves. They are zero at the rigid backing, Hence, one has

$$u^s_{dp}(z) = A\,\sin(k_1 z) + B\,\sin(k_2 z), \tag{8a}$$

$$u^t_{dp}(z) = A\mu_1\,\sin(k_1 z) + B\mu_2\,\sin(k_2 z). \tag{8b}$$

A and B are unknowns amplitudes. The *in-vacuo* stress and the pressure then read

$$\hat{\sigma}^s_{zz}(z) = P_{dp}\left[Ak_1\,\cos(k_1 z) + Bk_2\,\cos(k_2 z)\right], \tag{9a}$$

$$p(z) = -\widetilde{K}_{dp}\left[Ak_1\mu_1\,\cos(k_1 z) + Bk_2\mu_2\,\cos(k_2 z)\right]. \tag{9b}$$

At the air-porous interface ($z = -d$), the *in-vacuo* stress is zero. This condition allows finding the value of the ratio A/B (independent of P_{dp}). In addition, the normal total displacement (resp. pressure) is equal to the air displacement (resp. pressure). Hence,

$$Z_s^{dp} = \frac{p(z=-d^+)}{\mathrm{j}\omega u^t_{dp}(z=-d^+)} = \frac{\widetilde{K}_{dp}}{\mathrm{j}\omega}\times\frac{k_1k_2(\mu_2-\mu_1)}{k_1\mu_2\tan(k_2 d)-k_2\mu_1\tan(k_1 d)}, \tag{10}$$

with $\mathrm{j} = \sqrt{-1}$. Calculation of the absorption coefficient is then straightforward [26].

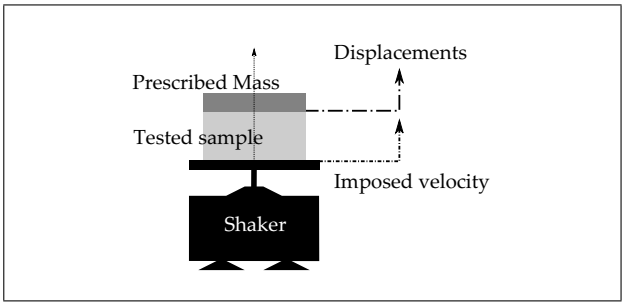

Figure 1. Configurations considered in the inversion procedure of solid parameters.

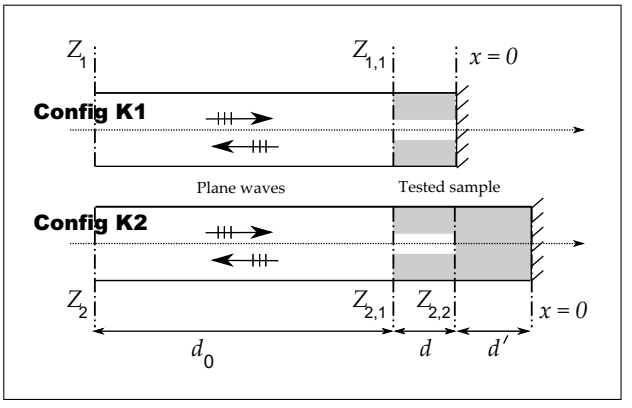

Figure 2. Configurations considered in the inversion procedure of fluid parameters.

3. Numerical inverse procedures

Two numerical inverse procedures (associated to problems depicted in Figure 1 and 2) are presented in this section. Their objective is to numerically deduce the acoustic and elastic parameters of the double porosity materials. First procedure corresponds to the uniaxial compression loading dynamic setup to determine P_{dp}. *In-vacuo* conditions are considered. The second problem is associated to Kundt tube measurements in two different configurations (denoted by $K1$ and $K2$ in Figure 2). $K1$ corresponds to a layer of double porosity material with thickness d bonded onto a rigid wall. $K2$ is similar to $K1$ but a porous layer of thickness d' is added between the double porosity material and the rigid backing. Note that a porous medium is considered instead of an air cavity (plenum) to avoid numerical discrepancies due to singularities of the cotangent

function. In the simulations, the double porosity layer is not homogenized and both microporous domain and the mesopore are simulated using the Finite-Element Method (FEM). From simulation of $K1$ and $K2$, it is shown that it is possible to deduce equivalent fluid properties of the double porosity. Note that other combinations of configurations could have been used inspired from [29]. The proposed configuration has been chosen as it appears very robust and does not need restriction on dimensions d and d'.

Three types of FE models have been implemented. The first one concerns the determination of the elastic parameters of the materials and is associated with a classical solid FE model. The second one is associated with porous structures that are assumed to be rigid and motionless (so-called equivalent fluid medium). It is denoted by eq-FEM. The third model is similar to the second one under the assumption that the porous medium has an elastic frame ; it is denoted Biot-FEM. For the sake of clarity, details of the FE model implementation are given in Appendix A1. Finally, it may be underlined that all FE computations have been performed using in house developed software and that all meshes have been generated using the FreeFEM software. The following two sections describe procedures for characterizing the elastic and damping parameters, and the procedure for determining the acoustic propagation characteristics in single porosity media.

3.1. Estimation of the mechanical parameters of the double porosity material. P_{dp}

Assuming uniform and identical strain in the skeleton and in the air contained in the perforation, it is possible to estimate the ratio τ of equivalent rigidities [30],

$$\tau = \frac{P_{dp}}{P} \simeq \left(1 - \phi_p\right). \tag{11}$$

The validity of this approximation is checked numerically. The uniaxial compression dynamic loading method has been proposed by Pritz [31] and used by several authors [32, 33, 34, 35, 36]. It is presented Figure 1. A sample of porous material is placed between a driving plate (Γ_m) of an electrodynamic shaker and a top plate (Γ_m) which acts as a mass (denoted m). If the mass of the porous sample is negligible compared to m, it behaves as a spring of stiffness $k = ES\alpha/h$, where E is the Young's modulus of the sample, S is the surface of the base of the sample, h is the thickness of the sample and α is a correction accounting for the Poisson effect ($\alpha = 1$ for fibrous materials see for example section 3.1 of reference [36]). Let $T(\omega)$ be the transmissibility defined [31] as the ratio of the top plate's displacement over the driving plate's one. One then has two different ways to evaluate E,

$$E \approx E_{res} = \frac{\omega_{res}^2 mh}{\alpha S},$$
$$E \approx E_\infty = \lim_{\omega\to\infty} -\frac{\omega^2 mhT(\omega)}{\alpha S}. \tag{12}$$

ω_{res} is the pulsation of the resonance frequency of the mass-spring system.

Table IV. Results of the mechanical inversion procedure.

DP material	$E_{dp}(kPa)$	$1-\phi_p$	τ_{res}
F	248.8	0.9573	0.9586
W1	4798	0.8724	0.867
W2	4449	0.809	0.808

DP material	τ_∞	ε_{res}	ε_∞
F	0.9572	0.2%	0.01%
W1	0.867	0.6%	0.6%
W2	0.802	0.17%	0.8%

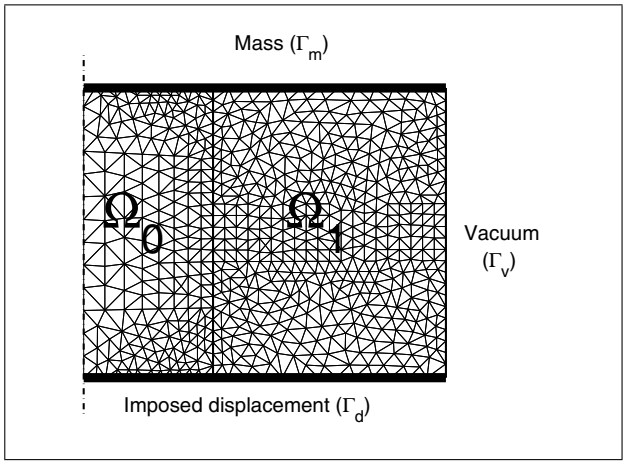

Figure 3. Configuration of the FE problem for the mechanical procedure.

Hence $T(\omega)$ is simulated by quadratic axisymmetric finite-elements (See Figure 3). In the case of single (Ω_0 and Ω_1 are fulfilled by the microporous material) and double (Ω_0 is vacuum) porosity material. One main advantage of the finite-element procedure is that one can overcome experimental constraints. In addition it is trivial to consider a *in-vacuo* problem and there is no bending of the top plate which is a classical drawback of the experimental setup. It is an advantage of numerical (i.e. virtual) experiments that most of the factors can be controlled. Transmissibility is presented Figure 4 for the fibrous and the double porosity material W1. The effect of the perforation tends to lower the resonance frequency of the mass-spring system.

For each material, ratios τ_{res} and τ_∞ are calculated. They correspond to the ratio (11) estimated at the resonance frequency and in the limit of high frequencies (determined as 5 times the resonance frequency). Results are presented Table IV and indicates that error are lower than 1%.

3.2. Determination of equivalent fluid parameters $\widetilde{\rho}_{dp}$ and $\widetilde{K}_{dp}$

In this section, the porous frame is assumed motionless. Therefore, the model used is eq-FEM. The double porosity material is supposed to be homogenized with characteristic impedance $Z_{dp} = \sqrt{\widetilde{\rho}_{dp}\widetilde{K}_{dp}}$ and wave number k_{dp}.

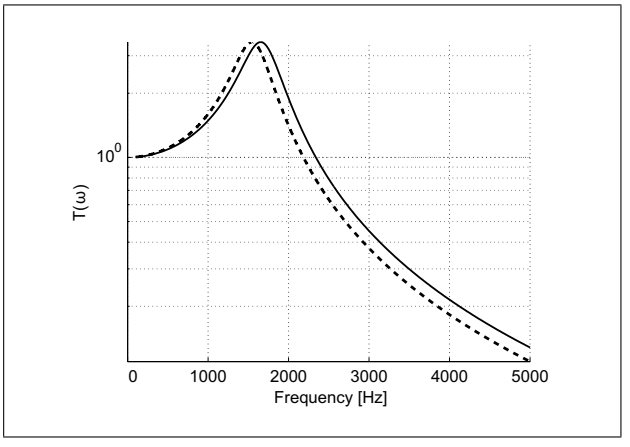

Figure 4. Transfer functions $T(\omega)$ simulated by FEM for the mechanical problem for W1; Solid : Single porosity material, Dashed: Double porosity material.

A layer of double porosity material is therefore similar to a fluid medium.

Impedances Z_1 and Z_2 associated with configurations $K1$ and $K2$ are first calculated. Assuming that the layers can be homogenized, the porous layer (resp. double porosity, air) is described by its characteristic impedance Z_{eq} (resp. Z_{dp}, Z_0) and wavenumber k_{eq} (resp. k_{dp}, k_0).

For both configurations ($k = 1, 2$), impedances at the surface of the double porosity layer $Z_{k,1}$ can be deduced from Z_k,

$$Z_{k,1} = Z_0 \frac{\mathrm{j}Z_0 - Z_k \cot(k_0 d_0)}{\mathrm{j}Z_k - Z_0 \, cot(k_0 d_0)}, \quad k = 1, 2. \tag{13}$$

Impedances $Z_{1,1}$ and $Z_{2,2}$ are given as

$$\begin{aligned} Z_{1,1} &= -\mathrm{j}Z_{dp} cot(k_{dp} d), \\ Z_{2,2} &= -\mathrm{j}Z_{eq} \cot(k_{eq} d'). \end{aligned} \tag{14}$$

For configuration 2, surface impedances are related as

$$Z_{2,2} = Z_{dp} \frac{\mathrm{j}Z_{dp} - Z_{2,1} \cot(k_{dp} d)}{\mathrm{j}Z_{2,1} - Z_{dp} \cot(k_{dp} d)}. \tag{15}$$

From the two above equations, we get

$$Z_{dp}^2 = Z_{2,1} Z_{1,1} - Z_{2,2}(Z_{1,1} - Z_{2,1}). \tag{16}$$

Z_{dp} is the square root with the positive real part and

$$k_{dp} = \frac{\operatorname{atan}\left(-\dfrac{\mathrm{j}Z_{dp}}{Z_{1,1}}\right)}{d} \tag{17}$$

The two quantities are computed at each frequency and the surface impedance (and then the absorption) is obtained using equation (14).

In order to validate the accuracy of the inversion procedure for double porosity materials, it has been tested for several experimental double porosity configurations. It is validated on the basis of comparisons with sound absorption data measured using the recommended standard ISO

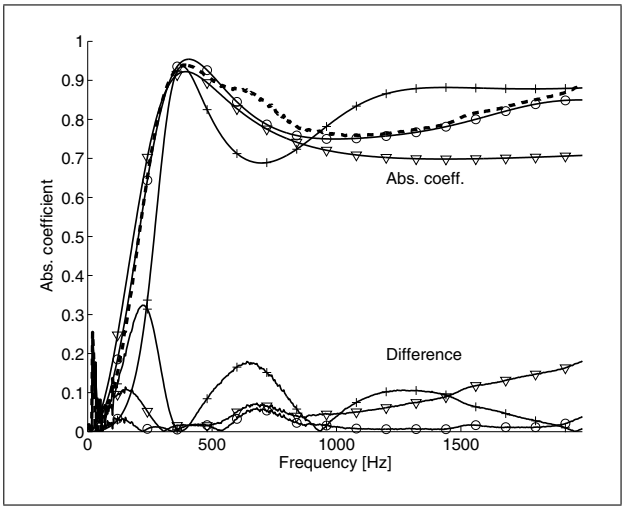

Figure 5. Sound absorption coefficient for material W1. '– –' Experiments, 'o' Inversion proposed model, '+' No diffusion double porosity model, '▽' Diffusion double porosity model.

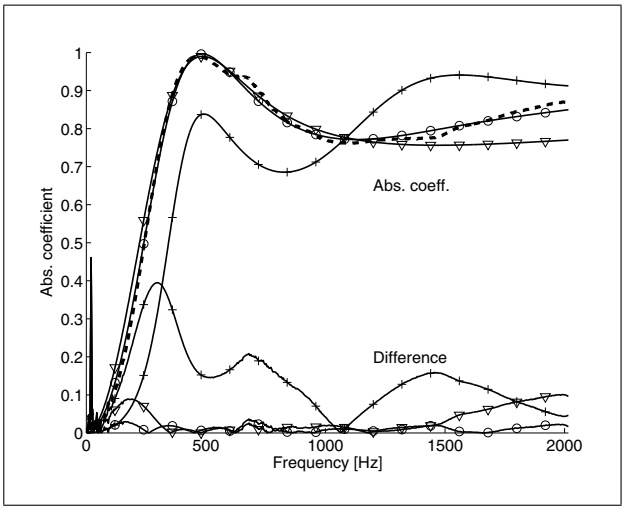

Figure 6. Normal incidence sound absorption coefficient for material W2. '- -' Experiments, 'o' Inversion proposed model, '+' No diffusion double porosity model, '▽' Diffusion double porosity model.

10534-2 [37] and with direct computations of sound absorption coefficients using the theory of Olny & Boutin [14] adapted to the present axisymmetric problem (the original theory was developed to circular mesopores in rectangular samples). For these latter calculations, denoted hereinafter semi-analytical models, pressure diffusion effects may also be accounted for. Two examples are given in Figure 5 and 6 respectively for the two fibrous materials W1 and W2.

To ease the analysis, discrepancies between the model predictions and the data ($\left|\alpha_{model} - \alpha_{exp}\right|$) are also given for the three models. Note that the effect of the solid frame deformation can be observed between 500 and 800 Hz and cannot be captured by the models considered in this section assume a rigid and motionless skeleton. The absorption peak observed in the measured data around 400 Hz

is associated to double porosity phenomena. The diffusion frequency [14] is estimated at 361 Hz for material W1 and at 498 Hz for material W2. Before this transition frequency, pressure diffusion effects shall be dominant and the semi-analytical model accounting for them should be used.

As expected, for the two materials tested here, and for the entire frequency range observed, this model allows a better prediction. Accordingly, the analytical model without diffusion effects fails to give accurate predictions.

Meanwhile, the results obtained with the inversion procedure proposed above agree with the measured data. Outside the frequency region where deformation of the skeleton dominates, the error associated to this procedure never exceeds a value of 0.05 on the absorption coefficient. Errors associated to the other two analytical models may locally reach 0.4 points of absorption. Note finally that the main difference between the two analytical models, which assume a material of infinite lateral extent, and the proposed procedure is that the latter technique allows capturing the acoustical effects due to the finite size of the sample. In fact, the deviations observed between these models are likely to be attributed to the influence of finite size on the pressure diffusion effects which could be captured when considering the actual geometry of the tested sample.

The solid resonance cannot be captured by the different models. That is the reason why the comparison between models and experiments shall not be performed in this frequency range. The model not accounting for pressure diffusion has a global error close to 0.1 averaged over the whole frequency range. It underestimates the absorption before the peak and presents a recurrent error after that. The diffusion model gives accurate results but overestimates the levels at the peak of absorption and presents small discrepancies for frequencies higher than 1500 Hz. The inversion procedure proposed in this paper allows finding the absorption with an error lower than 0.03 except in the frequency range where Biot effects are significant. Figure 6 presents results for W2. As the mesopore is larger, finite size effects are more important and noticeable discrepancies appear for the diffusion model.

4. Results for elastic frame double porosity materials

Models accounting for the porous frame deformations are now compared with experiments for three double porosity materials (F, W1 and W2). Results are presented in Figure 7 to 10. In each one of the following graphs, absorption curve are obtained through eq-FEM, Biot-FEM and analytically using expression (10). Inversion procedure has been used to obtain equivalent fluid parameters.

Figure 7 presents results for material W1. Solid frame resonance is in the 500-1000 Hz frequency range. A good agreement is obtained between the proposed analytical model (10) and experimental results. In particular, the proposed model captures the curve inflection observed in the measured data between 600 Hz and 800 Hz. Absorption

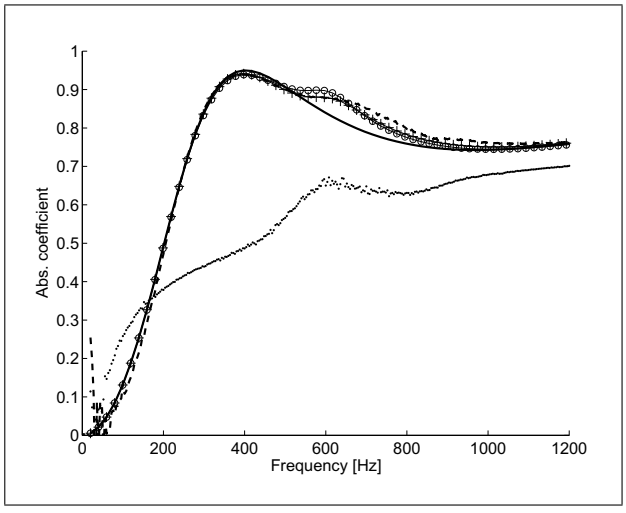

Figure 7. Normal incidence sound absorption coefficient for material W1; 'Solid': eq-FEM, 'o': 'Biot-FEM, '+': Semi-analytical proposed model, 'Dashed': Experimental data for DP material. 'Dotted': Experimental data for SP material.

levels at other frequencies remain the same as those predicted by the model of the previous section which assumed a rigid and motionless frame. Note that a little discrepancy is observed with Biot-FEM which is not significant and could be removed by adjusting the elastic parameters used in the FE model. This parameter tuning would correspond to the modifications of the effective elastic and damping properties of the sample when inserted inside the impedance tube. Absorption coefficient is only concerned with the modulus of the reflection coefficient. In order to illustrate that the model is also able to capture informations relative to the the complex nature of the reflection, Figure 8 presents its phase. A very good agreement is observed. Not that to fit the simulations a correction (2.5 mm) of the tube length should have been proceeded. This correction is compatible with the uncertainties of the experimental setup. For material W2, presented Figure 9, the proposed model also shows to be robust and compares well with the Biot-FEM model and measured data. For the foam, material F, results are presented Figure 10. Biot effects are noticeable on the entire frequence range. Therefore, for this material, the eq-FEM is not suited to model the absorption correctly. The proposed semi-analytical model predicts the frame resonance and the correspondence between its prediction and the measured data is satisfactory. Note finally that, for this double porosity material, the estimated diffusion frequency is 748 Hz and that pressure diffusion should no longer be visible at high frequencies.

5. Conclusion

In this work the adaptation of the Biot theory is proposed to model sound propagation in double porosity material accounting for possible frame deformation. The main idea is to replace the fluid properties of the single porosity material by those of the double porosity medium. A simplified

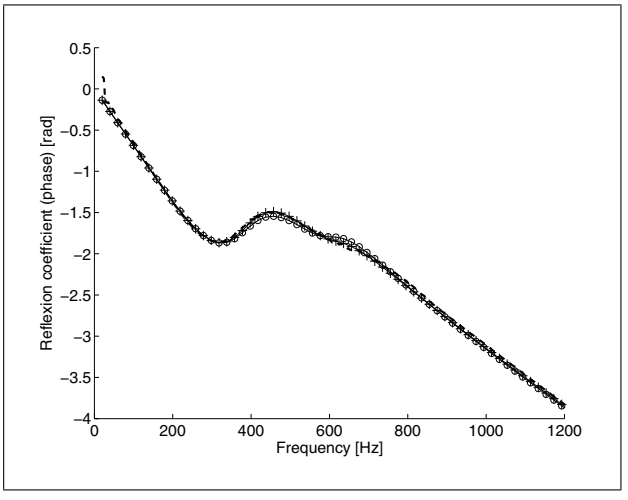

Figure 8. Phase of the reflection coefficient for material W1; 'Solid': eq-FEM, 'o': 'Biot-FEM, '+': Semi-analytical proposed model, 'Dashed': Experimental data.

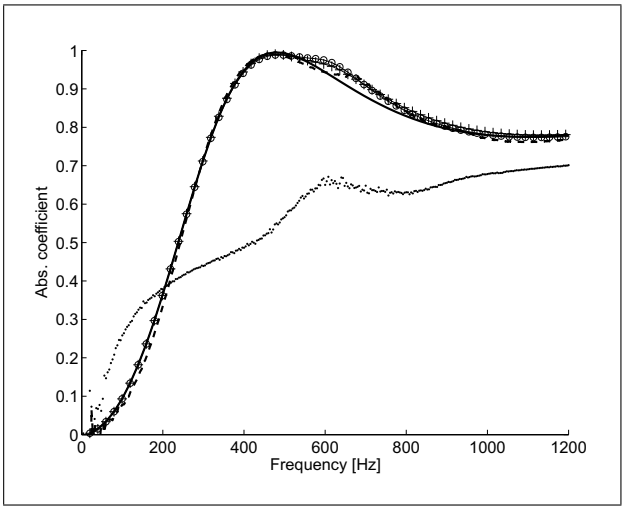

Figure 9. Absorption coefficient for material W2; 'Solid': eq-FEM, 'o': 'Biot FEM, '+': Semi-analytical proposed model, 'Dashed': Experimental data.

one-dimensional model was derived. Its predictions for the normal incidence surface impedance have been compared with impedance tube measurements.

New approaches to the inverse numerical procedures based on Finite-Element simulations to determine the values of the model's parameters have been proposed in this work. Procedure takes account for possible modifications of the pressure diffusion effects for samples of laterally finite thickness.

Comparisons with sound absorption measurements on three different materials (fibrous and foam) have proved that the model is able to describe the combined acoustic effects due to the presence of double porosity as well as the porous frame deformation.

Further works involves extension of the validation of the model for oblique incidence. It could also be interesting to check if criteria to check the validity of the limp model [38, 39] for equivalent fluid remain valid. In addition, this

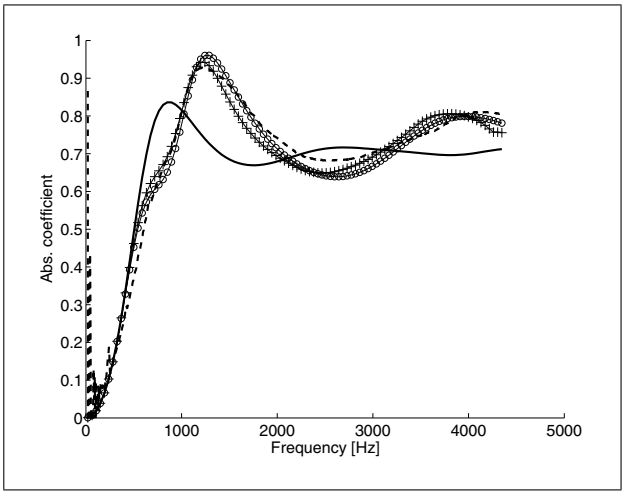

Figure 10. Absorption coefficient for material F; 'Solid': eq-FEM, 'o': 'Biot-FEM, '+': Semi-analytical proposed model, 'Dashed': Experimental data for DP material. 'Dotted': Experimental data for SP material.

work has demonstrated the limitation of double porosity models in the case of finite size samples and the need of their extension as alternatives to FE computations.

Appendix

A1. Finite-Elements models

FE models [40] for configurations $K1$ and $K2$ are presented Figure A1. The problem is axisymmetric of axis (AB) and the figure represents only half (right hand side) of the complete tested sample. AD= Γ_e is the excitation boundary. BC= Γ_b corresponds to a rigid backing. CD= Γ_t corresponds to the tube wall. The fluid normal displacement is equal to 0 on these three boundaries. Ω_0 is an air layer which is introduced into the model so as to take into account evanescent modes which may result from the presence of the perforation in double porosity materials. . Ω_1 corresponds to the microporous domain. Ω_2 is the perforation and is fulfilled by air. Ω_3 is porous domain with rigid and motionless frame which is considered in configuration $K2$. In configuration $K1$, Ω_3 is removed. . The domain is meshed through a Delaunay procedure so as to ensure a $\lambda/9$ convergence criterion and so as each triangle of the mesh belongs to only one Ω_i. Convergence of the model has been checked and it appears that this criterion is sufficient.

Two types of simulations were performed depending on the assumption made for the porous domain Ω_1. In the eq-FEM model, the porous frame is assumed to be infinitely rigid and motionless while in the Biot-FEM model possible frame deformation are accounted for.

In the case of eq-FEM, each domain is associated with a fluid and the variational formulation reads

$$\forall q \in H^1(\Omega), \qquad \text{(A1)}$$
$$\int_\Omega \frac{1}{\rho_i \omega^2} \nabla p \, \nabla q \, - \frac{1}{K_i} pq \, \mathrm{d}\Omega = - \oint_{\partial\Omega} \frac{1}{\rho_i} \frac{\partial p}{\partial n} q \, \mathrm{d}\Gamma.$$

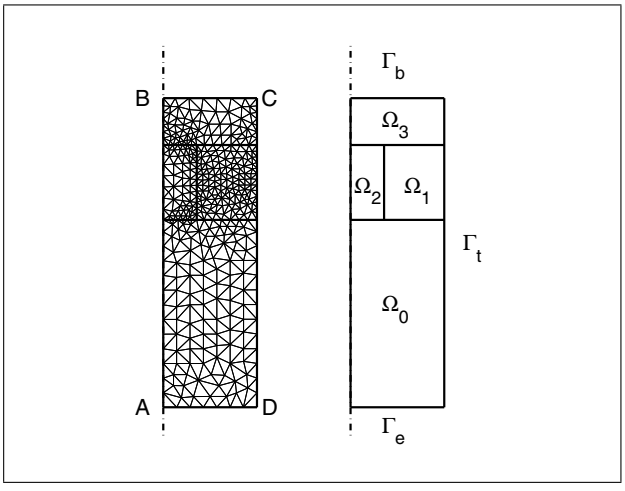

Figure A1. Configuration of the finite element model for the impedance tube problem.

ρ_i and K_i are respectively the density and the compressibility of the equivalent medium (as an example: $\rho_i = \rho_0$ in $\Omega_0 \cup \Omega_2$ and $\rho_i = \widetilde{\rho}_{eq}$ in $\Omega_1 \cup \Omega_3$). The boundary integral of the right hand side is non null on Γ_0 which is associated with the excitation. It has been checked on the simulation results that the pressure field on Γ_0 is only slightly varying and the distance d_0 is enough to remove the influence of the evanescent modes. On Γ_0, one has

$$P_{|\Gamma_0} = 1 + R, \qquad \text{(A2)}$$
$$\oint_{\Gamma_0} \frac{1}{\rho_i} \frac{\partial p}{\partial n} q d\Gamma = \frac{k_0}{\rho_0}(1-R) \oint_{\Gamma_0} q \, \mathrm{d}\Gamma.$$

It is proposed to directly calculate R by adding this parameter to the degrees of freedom of the problem. After discretization the boundary integral can be expressed in the form

$$\frac{k_0}{\rho_0}\big(1-R\big) \oint_{\Gamma_0} q \, \mathrm{d}\Gamma \;\Rightarrow\; \mathbf{B}\big(1-R\big), \qquad \text{(A3)}$$

where $\mathbf{B}$ is a $n \times 1$ vector. It is necessary to add an additional equation associated to the pressure continuity condition on the boundary. Let $\mathbf{B}'$ be the $1 \times n$ boolean vector whose unique non-null value corresponds to the degree of freedom associated to the pressure at point A.

The final system set of equations is then of size $n + 1$ and reads

$$\left[\begin{array}{c|c} \frac{1}{\omega^2}[\widetilde{\mathbf{H}}] - [\widetilde{\mathbf{Q}}] & \mathbf{B} \\ \hline \mathbf{B}' & -1 \end{array}\right] \left\{\begin{array}{c} \mathbf{P} \\ R \end{array}\right\} = \left\{\begin{array}{c} \mathbf{B} \\ 1 \end{array}\right\} \qquad \text{(A4)}$$

$[\widetilde{H}]$ and $[\widetilde{Q}]$ represent the kinetic and compression energy matrices of the fluid phase. The reflection coefficient is thereby directly calculated. Surface impedance and/or absorption coefficient can be deduced by classical relations.

Biot-FEM is obtained in a similar manner. Ω_1 is modeled by a Biot $\{u, p\}$ classical formulation [41]. Solid displacement $\{u_r, u_z\}$ should be added to the degrees of freedom. In Ω_1 the variational formulation now reads

$$\forall v \in H^1(\Omega)^3,$$
$$\int_{\Omega_1} \hat{\boldsymbol{\sigma}}^s(u) : \boldsymbol{\varepsilon}(v) - \omega^2 \widetilde{\rho} u \cdot \mathbf{v} - \widetilde{\gamma} \nabla \mathbf{p} \cdot \mathbf{v} \mathrm{d}\boldsymbol{\Omega}$$
$$= \oint_{\partial\Omega_1} \big[\hat{\boldsymbol{\sigma}}^s(u) \cdot n\big] v \, \mathrm{d}\Gamma \qquad \text{(A5)}$$

$$\forall q \in H^1(\Omega),$$
$$\int_{\Omega_1} \left[\frac{\nabla p \, \nabla q}{\widetilde{\rho}_{eq}\omega^2} - \frac{pq}{\widetilde{K}_{eq}} - \widetilde{\gamma} u . \nabla q\right] \mathrm{d}\Omega$$
$$= \oint_{\partial\Omega_1} \left[\widetilde{\gamma} u_n - \frac{1}{\widetilde{\rho}_{eq}} \frac{\partial p}{\partial n}\right] q \, \mathrm{d}\Gamma. \qquad \text{(A6)}$$

As Biot $\{u, p\}$ formulation allows coupling of the contiguous fluid domains naturally, the surface integrals at the interfaces between the different subdomains are all vanishing. Sliding conditions are considered on Γ_t. The procedure to calculate the reflection coefficient remains unchanged as the porous structure is not directly connected to Γ_0. One finally has

$$\left[\begin{array}{cc|c} [\widetilde{\mathbf{K}}] - \omega^2[\widetilde{\mathbf{M}}] & [\widetilde{\mathbf{C}}] & \mathbf{0} \\ [\widetilde{\mathbf{C}}]^t & \frac{1}{\omega^2}[\widetilde{\mathbf{H}}] - [\widetilde{\mathbf{Q}}] & \mathbf{B} \\ \hline \mathbf{0} & \mathbf{B}' & -1 \end{array}\right] \left\{\begin{array}{c} \mathbf{u} \\ \mathbf{P} \\ R \end{array}\right\} = \left\{\begin{array}{c} \mathbf{0} \\ \mathbf{B} \\ 1 \end{array}\right\} \qquad \text{(A7)}$$

$[\widetilde{\mathbf{K}}]$and $[\widetilde{\mathbf{M}}]$ represent the stiffness and mass matrices of the solid phase. They are square matrices of size n_u which correspond to the number of displacement degrees of freedom. It should be noticed that $[\widetilde{\mathbf{C}}]$ coupling matrix is of size $n \times n_u$ but all the columns associated to pressure degrees of freedom which are not in Ω_1 are null. R is then calculated so as to deduce surface impedances and absorption coefficients[26].

References

[1] B. Brouard, D. Lafarge, J.-F. Allard: A general method of modelling sound propagation in layered media. J. Sound Vib. **183** (1995) 129–142.

[2] M.-L. Munjal: Response of a multi-layered infinite plate to an oblique plane wave by means of transfer matrices. Journal of Sound and Vibration **162** 333–343.

[3] P. Guignouard, M. Meisser, J.-F. Allard, P. Rebillard, C. Depollier: Prediction and measurement of the acoustical impedance and absorption coefficient at oblique incidence of porous layers with perforated facings. Noise Control Engineering **36** (1991) 129–135.

[4] U. Ingard: Perforated facing and sound absorption. J. Acoust. Soc. Am. **26** (1954).

[5] N. Atalla, F. Sgard: Modeling of perforated plates and screens usig rigid frame porous models. Journal of Sound and Vibration **303** (2007) 195–208.

[6] M. Furstoss, D. Thenail, M. A. Galland: Surface impedance control for sound absorption: direct and hybrid passiv / active strategies. Journal of Sound and Vibration **203** (1997) 219–236.

[7] M. A. Galland, B. Mazeaud, N. Sellen: Hybrid passive / active absorbers for flow ducts. Applied Acoustics **66** (2005) 691–708.

[8] P. Leroy, N. Atalla, A. Berry, P. Herzog: Three dimensional finite element modeling of smart foam. J. Acoust. Soc. Am. **126** (2009) 2873.

[9] C. Boutin, P. Royer, J. L. Auriault: Sound absorption of dry porous media with single and double porosity. Journal of Engineering Mechanics (1995) 796–799.

[10] J. L. Auriault, C. Boutin: Deformable media with double porosity - quastistatics. I: Coupling efects. Transport in porous media **7** (1992) 63–82.

[11] J. L. Auriault, C. Boutin: Deformable media with double porosity - quastistatics. II: Memory effects. Transport in porous media **10** (1993) 153–159.

[12] J. L. Auriault, C. Boutin: Deformable media with double porosity. III. Acoustics. Transport in porous media **14** (1994) 143–162.

[13] C. Boutin, P. Royer, J. L. Auriault: Acoustic absorption of porous surfacing with dual porosity. International Journal of Solids Structures **35** (1998) 4709–4737.

[14] X. Olny, C. Boutin: Acoustic wave propagation in double porosity media. J. Acoust. Soc. Am. **114** (2003) 73–89.

[15] N. Atalla, F. Sgard, X. Olny, R. Panneton: Acoustic absorption of macro-perforated porous materials. Journal of Sound and Vibration **243** (2001) 659–678.

[16] F. C. Sgard, X. Olny, N. Atalla, F. Castel: On the use of perforations to improve the sound absorption of porous materials. Applied Acoustics **66** (2005) 625–651.

[17] F.-X. Bécot, L. Jaouen, E. Gourdon: Application of the dual porosity theory to irregularly shaped porous materials. Acta Acust united with Acustica **94** (2008) 715–724.

[18] E. Sanchez-Palencia: Non-homogeneous media and vibration theory. 1980.

[19] J. Auriault, L. Borne, R. Chambon: Dynamics of porous saturated media, checking of the generalized law of Darcy. J. Acoust. Soc. Am. **77** (1985) 1641–1650.

[20] X. Olny: Acoustical properties of multiscales absorbing porous materials. Proceedings of SAPEM, Lyon, France, December 7-9, 2005.

[21] X. Olny: Absorption acoustique des milieux poreux à simple et double porosité. modélisation et validation expérimentale (Acoustic absorption of porous media with single and double porosity–modeling and experimental validation). Ph.D. thesis, INSA-Lyon, 1999.

[22] R. Panneton: Comments on the limp frame equivalent fluid model for porous media. J. Acoust. Soc. Am. **122** (2007) EL217–EL222.

[23] M. A. Biot: Theory of propagation of elastic waves in a fluid-filled-saturated porous solid. I. Low-frequency range. J. Acoust. Soc. Am. **28** (1956) 168–191.

[24] M. A. Biot: Mechanics of deformation and acoustic propagation in porous media. Journal of Applied Physics **33** (1962) 1482–1498.

[25] J.-F. Allard, C. Depollier, A. L'Esperance: Observation of the Biot slow waves in a foam of high flow resistance at acoustic frequencies. Journal of Applied Physics **56** (1986) 3367–3370.

[26] J.-F. Allard, N. Atalla: Propagation of sound in porous media-modelling sound absorbing materials. Wiley and Sons, 2009.

[27] O. Dazel, B. Brouard, C. Depollier, S. Griffiths: An alternative Biot's displacement formulation for porous materials. J. Acoust. Soc. Am. **121** (2007) 3509–3516.

[28] P. Khurana, L. Boeckx, W. Lauriks, P. Leclaire, O. Dazel, J.-F. Allard: A description of transversely isotropic sound absorbing porous materials by transfer matrices. J. Acoust. Soc. Am. **125** (2009) 915–921.

[29] C. D. Smith, T. L. Parrott: Comparison of three methods for measuring acoustic properties of bulk materials. J. Acoust. Soc. Am. **74** (1983) 1577–1582.

[30] J.-M. Berthelot: Composite materials: Mechanical behavior and structural analysis. 1998, Chap. 9.

[31] T. Pritz: Frequency dependence of frame dynamic characteristics of mineral and glass wool materials. Journal of Sound and Vibration **106** (1986) 161–169.

[32] M. Etchessahar, S. Sahraoui, L. Benyahia, J. F. Tassin: Frequency dependence of elastic properties of acoustic foams. J. Acoust. Soc. Am. **117** (2005) 1114.

[33] C. Langlois, R. Panneton, N. Atalla: Polynomial relations for quasi-static mechanical characterization of isotropic poroelastic materials. J. Acoust. Soc. Am. **110** (2001) 3032.

[34] O. Danilov, F. Sgard, X. Olny: On the limits of an "in vacuum" model to determine the mechanical parameters of isotropic poroelastic materials. Journal of Sound and Vibration **276** (2004) 729–754.

[35] N. Geebelen, L. Boeckx, G. Wermeir, J.-F. A. W. Lauriks, O. Dazel: Measurement of the rigidity coefficients of a melamine foam. Acta Acustica united with Acustica **93** (2007) 783–788.

[36] L. Jaouen, A. Renault, M. Deverge: Elastic and damping characterizations of acoustical porous materials: Available experimental methods and applications to a melamine foam. Applied Acoustics **69** (2008) 1129–1140.

[37] International Organization for Standardization: Acoustics - Determination of sound absorption coefficient and impedance in impedance tubes - Part 2: Transfer-function method. 1991, 27.

[38] O. Doutres, N. Dauchez, J. M. Genevaux, O. Dazel: Validity of the limp model for porous materials: A criterion based on the Biot theory. J. Acoust. Soc. Am. **122** (2007) 2038–2048.

[39] O. Doutres, N. Dauchez, J. M. Genevaux, O. Dazel: A frequency independent criterion for describing sound absorbing materials by a limp frame model. Acta Acustica united with Acustica **95** (2009) 178–181.

[40] O.-C. Zienckiewicz: The finite element method. Fourth edition, 2 volumes. Mc GrawHill, 1989.

[41] N. Atalla, R. Panneton, P. Debergue: A mixed displacement-pressure formulation for poroelastic materials. J. Acoust. Soc. Am. **104** (1998) 1444–1452.